sarcoma lesions. Therefore, cytotoxic T lymphocyte activity specific for HHV-8 proteins is a major pathway for the regression of Kaposi's sarcoma. In future, infusion of HHV-8 specific cytotoxic T lymphocytes, generated *in vitro* by incubating lymphocytes with irradiated HHV-8 infected cells in the presence of interleukin 2, might also be used. Similar cellular therapies have been effective for treatment of EBV related malignancy.

REFERENCES

1. Antman K, Chang Y. Kaposi's sarcoma. N Engl J Med 2000;342: 1027-1038.
2. Ballestas ME, Chatis PA, Kaye KM. Efficient persistence of extrachromosomal KSHV DNA mediated by latency-associated nuclear antigen. Science 1999;284:641-644.
3. Boivin G, Gaudreau A, Routy JP. Evaluation of the human herpesvirus 8 DNA load in blood and Kaposi's sarcoma skin lesions from AIDS patients on highly active antiretroviral therapy. AIDS 2000;14:1907-1910.
4. Boivin G, Gaudreau A, Toma E, Lalonde R, Routy JP, Murray G, Handfield J, Bergeron MG. Human herpesvirus 8 DNA load in leukocytes of human immunodeficiency virus-infected subjects: correlation with the presence of Kaposi's sarcoma and response to anticytomegalovirus therapy. Antimicrob Agents Chemother 1999;43:377-380.
5. Bower M, Fife K, Landau D, Gracie F, Phillips RH, Gazzard BG. Phase II trial of 13-cis-retinoic acid for poor risk HIV-associated Kaposi's sarcoma. Int J STD AIDS 1997;8:518-521.
6. Bower M, Fox P, Fife K, Gill J, Nelson M, Gazzard B. Highly active anti-retroviral therapy (HAART) prolongs time to treatment failure in Kaposi's sarcoma. AIDS 1999;13:2105-2111.
7. Cannon JS, Hamzeh F, Moore S, Nicholas J, Ambinder RF. Human herpesvirus 8-encoded thymidine kinase and phosphotransferase homologues confer sensitivity to ganciclovir. J Virol 1999;73:4786-4793.
8. Chang Y, Cesarman E, Pessin MS, Lee F, Culpepper J, Knowles DM, Moore PS. Identification of herpesvirus-like DNA sequences in AIDS-associated Kaposi's sarcoma. Science 1994;266:1865-1869.
9. Corbellino M, Bestetti G, Scalamogna C, Calattini S, Galazzi M, Meroni L, Manganaro D, Fasan M, Moroni M, Galli M, Parravicini C. Long-term remission of Kaposi sarcoma-associated herpesvirus-related multicentric Castleman disease with anti-CD20 monoclonal antibody therapy. Blood 2001;98: 3473-3475.
10. de Wit R, Danner SA, Bakker PJ, Lange JM, Eeftinck Schattenkerk JK, Veenhof CH. Combined zidovudine and interferon-alpha treatment in patients with AIDS-associated Kaposi's sarcoma. J Intern Med 1991;229:35-40.
11. de Wit R, Schattenkerk JK, Boucher CA, Bakker PJ, Veenhof KH, Danner SA. Clinical and virological effects of high-dose recombinant interferon-alpha in disseminated AIDS-related Kaposi's sarcoma. Lancet 1988;2:1214-1217.
12. Dittmer D, Stoddart C, Renne R, Linquist-Stepps V, Moreno ME, Bare C, McCune JM, Ganem D. Experimental transmission of Kaposi's sarcoma-associated herpesvirus (KSHV/HHV-8) to SCID-hu Thy/Liv mice. J Exp Med 1999;190:1857-1868.
13. Gill PS, Espina BM, Moudgil T, Kidane S, Esplin JA, Tulpule A, Levine AM. All-trans retinoic acid for the treatment of AIDS-related Kaposi's sarcoma: results of a pilot phase II study. Leukemia 1994;8:S26-32.
14. Gill PS, Lunardi-Ishkandar Y, Louie S, Tulpule A, Zheng T, Espina BM, Besnier JM, Hermans P, Levine AM, Bryant JL, Gallo RC. The effects of preparations of human chorionic gonadotropin on AIDS-related Kaposi's sarcoma. N Engl J Med 1996;335:1261-1269.
15. Gill PS, Rarick M, McCutchan JA, Slater L, Parker B, Muchmore E, Bernstein-Singer M, Akil B, Espina BM, Krailo M, et al. Systemic treatment of AIDS-related Kaposi's sarcoma: results of a randomized trial. Am J Med 1991;90:427-433.
16. Gustafson EA, Schinazi RF, Fingeroth JD. Human herpesvirus 8 open reading frame 21 is a thymidine and thymidylate kinase of narrow substrate specificity that efficiently phosphorylates zidovudine but not ganciclovir. J Virol 2000;74:684-692.
17. Kaposi M. Idiopatiches multiples pigment sarcom der Haut. Arch Dermatol Syphil 1872;4:265-272.
18. Katano H, Iwasaki T, Baba N, Terai M, Mori S, Iwamoto A, Kurata T, Sata T. Identification of antigenic proteins encoded by human herpesvirus 8 and seroprevalence in the general population and among patients with and without Kaposi's sarcoma. J Virol 2000;74:3478-3485.
19. Katano H, Sato Y, Kurata T, Mori S, Sata T. Expression and localization of human herpesvirus 8-encoded proteins in primary effusion lymphoma, Kaposi's sarcoma, and multicentric Castleman's disease. Virology 2000;269:335-344.
20. Kedes DH, Ganem D. Sensitivity of Kaposi's sarcoma-associated herpesvirus replication to antiviral drugs. Implications for potential therapy. J Clin Invest 1997;99:2082-2086.
21. Lane HC, Kovacs JA, Feinberg J, Herpin B, Davey V, Walker R, Deyton L, Metcalf JA, Baseler M, Salzman N, et al. Anti-retroviral effects of interferon-alpha in AIDS-associated Kaposi's sarcoma. Lancet 1988;2:1218-1222.
22. Lunardi-Iskandar Y, Bryant JL, Zeman RA, Lam VH, Samaniego F, Besnier JM, Hermans P, Thierry AR, Gill P, Gallo RC. Tumorigenesis and metastasis of neoplastic Kaposi's sarcoma cell line in immunodeficient mice blocked by a human pregnancy hormone. Nature 1995;375:64-68.
23. Martin DF, Kuppermann BD, Wolitz RA, Palestine AG, Li H, Robinson CA. Oral ganciclovir for patients with cytomegalovirus retinitis treated with a ganciclovir implant. Roche Ganciclovir Study Group. N Engl J Med 1999;340:1063-1070.
24. Mocroft A, Youle M, Gazzard B, Morcinek J, Halai R, Phillips AN. Anti-herpesvirus treatment and risk of Kaposi's sarcoma in HIV infection. Royal Free/Chelsea and Westminster Hospitals Collaborative Group. AIDS 1996;10:1101-1105.
25. Moore PS, Chang Y. Kaposi's sarcoma-associated herpesvirus. 4th ed. Fields Virology. Philadelphia: Lippincott Williams & Wilkins; 2001.
26. Nador RG, Cesarman E, Chadburn A, Dawson DB, Ansari MQ, Sald J, Knowles DM. Primary effusion lymphoma: a distinct clinicopathologic entity associated with the Kaposi's sarcoma-associated herpes virus. Blood 1996;88:645-656.
27. Neyts J, De Clercq E. Antiviral drug susceptibility of human herpesvirus 8. Antimicrob Agents Chemother 1997;41:2754-2756.
28. Northfelt DW, Dezube BJ, Thommes JA, Miller BJ, Fischl MA, Friedman-Kien A, Kaplan LD, Du Mond C, Mamelok RD, Henry DH. Pegylated-liposomal doxorubicin versus doxorubicin, bleomycin, and vincristine in the treatment of AIDS-related Kaposi's sarcoma: results of a randomized phase III clinical trial. J Clin Oncol 1998;16:2445-2451.
29. Opravil M, Hirschel B, Bucher HC, Luthy R. A randomized trial of interferon-alpha2a and zidovudine versus bleomycin and zidovudine for AIDS-related Kaposi's sarcoma. Swiss HIV

Cohort Study. Int J STD AIDS 1999;10:369-375.
30. Osman M, Kubo T, Gill J, Neipel F, Becker M, Smith G, Weiss R, Gazzard B, Boshoff C, Gotch F. Identification of human herpesvirus 8-specific cytotoxic T-cell responses. J Virol 1999;73:6136-6140.
31. Parravicini C, Chandran B, Corbellino M, Berti E, Paulli M, Moore PS, Chang Y. Differential viral protein expression in Kaposi's sarcoma-associated herpesvirus-infected diseases: Kaposi's sarcoma, primary effusion lymphoma, and multicentric Castleman's disease. Am J Pathol 2000;156:743-749.
32. Renne R, Zhong W, Herndier B, McGrath M, Abbey N, Kedes D, Ganem D. Lytic growth of Kaposi's sarcoma-associated herpesvirus (human herpesvirus 8) in culture. Nat Med 1996;2: 342-346.
33. Robles R, Lugo D, Gee L, Jacobson MA. Effect of antiviral drugs used to treat cytomegalovirus end-organ disease on subsequent course of previously diagnosed Kaposi's sarcoma in patients with AIDS. J Acquir Immune Defic Syndr Hum Retrovirol 1999;20:34-38.
34. Saville MW, Lietzau J, Pluda JM, Feuerstein I, Odom J, Wilson WH, Humphrey RW, Feigal E, Steinberg SM, Broder S, et al. Treatment of HIV-associated Kaposi's sarcoma with paclitaxel. Lancet 1995;346:26-28.
35. Soler RA, Howard M, Brink NS, Gibb D, Tedder RS, Nadal D. Regression of AIDS-related Kaposi's sarcoma during therapy with thalidomide. Clin Infect Dis 1996;23:501-503; discussion 504-505.
36. Soulier J, Grollet L, Oksenhendler E, Cacoub P, Cazals-Hatem D, Babinet P, d'Agay MF, Clauvel JP, Raphael M, Degos L, Sigaux F. Kaposi's sarcoma-associated herpesvirus-like DNA sequences in multicentric Castleman's disease. Blood 1995;86: 1276-1280.
37. Stewart S, Jablonowski H, Goebel FD, Arasteh K, Spittle M, Rios A, Aboulafia D, Galleshaw J, Dezube BJ. Randomized comparative trial of pegylated liposomal doxorubicin versus bleomycin and vincristine in the treatment of AIDS-related Kaposi's sarcoma. International Pegylated Liposomal Doxorubicin Study Group. J Clin Oncol 1998;16:683-691.
38. Suda T, Katano H, Delsol G, Kakiuchi C, Nakamura T, Shiota M, Sata T, Higashihara M, Mori S. HHV-8 infection status of AIDS-unrelated and AIDS-associated multicentric Castleman's disease. Pathol Int 2001;51:671-679.
39. Torre-Cisneros J, Pozo F, Serrano R, Vidal E, Rivero A, Tenorio A. Patterns of lymphotropic herpesvirus viraemia in HIV-infected patients with Kaposi's sarcoma treated with highly active antiretroviral therapy and liposomal daunorubicin. AIDS 2000;14:2215-2217.
40. Wit FW, Sol CJ, Renwick N, Roos MT, Pals ST, van Leeuwen R, Goudsmit J, Reiss P. Regression of AIDS-related Kaposi's sarcoma associated with clearance of human herpesvirus-8 from peripheral blood mononuclear cells following initiation of antiretroviral therapy. AIDS 1998;12:218-219.

Virus Genes 21:3, 237–247, 2003

Latency-Associated Nuclear Antigen of Kaposi's Sarcoma-Associated Herpesvirus Interacts with Human Myeloid Cell Nuclear Differentiation Antigen Induced by Interferon α

MASAYA FUKUSHI,[1] MASAYA HIGUCHI,[1] MASAYASU OIE,[1] TAKAFUMI TETSUKA,[1,2] FRANCIS KASOLO,[3] KOUJI ICHIYAMA,[3,4] NAOKI YAMAMOTO,[4] HARUTAKA KATANO,[5] TETSUTARO SATA[5] & MASAHIRO FUJII[1,*]

[1]*Division of Virology,* [2]*Division of Clinical Nephrology, Rheumatology, Respiratory Medicine and Infection Control and Prevention, Niigata University Graduate School of Medical and Dental Sciences, 1-757, Asahimachi-Dori, Niigata, 951-8510, Japan*
[3]*Virology Laboratory, Department Pathology and Microbiology, University Teaching Hospital, P/Bag RW 1X, Lusaka, Zambia*
[4]*Department of Molecular Virology, Division of Infection and Bioresponse Graduate School, Tokyo Medical and Dental University, 1-5-45 Yushima, Bunkyo-ku, Tokyo, 113-8519, Japan*
[5]*Department of Pathology, National Institute of Infectious Diseases, 1-23-1 Toyama, Shinjyuku-ku, Tokyo, 162-8640, Japan*

Revised May 27, 2003; Accepted June 11, 2003

Abstract. Kaposi's sarcoma-associated herpesvirus (KSHV)/human herpes virus type 8 (HHV-8) is tightly linked to the development of Kaposi's sarcoma, primary effusion lymphoma (PEL) and some cases of multicentric Castleman's disease. Latency-associated nuclear antigen (LANA) is one of a limited number of KSHV genes consistently expressed in these diseases as well as in KSHV-infected cell lines derived from PEL, and has been shown to play crucial role in persistence of KSHV genomes in the infected cells. In this study, we explored the cellular factors that interact with LANA using yeast two-hybrid screening, and isolated a part of gene encoding human myeloid cell nuclear differentiation antigen (MNDA). MNDA is a hematopoietic interferon-inducible nuclear proteins with a HIN-200 family member with conserved 200-amino acid repeats. Immunoprecipitation assay revealed that LANA interacted with MNDA in a mammalian embryonic kidney cell line. *MNDA* transcript was undetectable in three PEL cell lines by reverse-transcription polymerase chain reaction, but it was induced by interferon α (IFNα). Moreover, LANA and MNDA were co-localized in the nuclei of *MNDA*-expressing PEL cells. Our results suggest that LANA interacts with MNDA in KSHV-infected cells exposed to IFNα. Such interaction may modulate IFN-mediated host defense activities.

Key words: HIN-200 family genes, human myeloid cell nuclear differentiation antigen (MNDA), interferon (IFN), Kaposi's sarcoma-associated herpesvirus (KSHV)/human herpesvirus 8 (HHV-8), latency-associated nuclear antigen (LANA), yeast two-hybrid screening

Introduction

Kaposi's sarcoma-associated herpesvirus (KSHV), also called as human herpesvirus 8 (HHV-8), was isolated from a tumor tissue of a patient with Kaposi's sarcoma (KS) associated with acquired immunodeficiency syndrome (AIDS) [1]. Subsequent studies have shown that KSHV infection is tightly linked to the development of KS associated with or without AIDS. KSHV has also been implicated in lymphoproliferative disorders, including primary effusion lymphoma (PEL) and some cases of multicentric Castleman's disease [2–5].

Kaposi's sarcoma-associated herpesvirus establishes a latent infection in KS spindle cells as well as in cell lines derived from PEL [6]. During latent infection, a limited number of KSHV genes are expressed in the KSHV-infected cell. One of them is the latency-associated nuclear antigen (LANA) [7–9].

* Author for all correspondence.
E-mail: fujiimas@med.niigata-u.ac.jp

LANA was originally identified as a major viral antigen in a PEL cell line by an immunofluorescence assay using sera from KS patients [10–12]. Subsequent studies showed that LANA is encoded by open reading frame 73 of the KSHV genome, and it is a nuclear protein consisting of 1,162 amino acids [9,13].

Accumulating evidence indicates that LANA plays crucial role in replication and maintenance of the viral episomal genomes in KSHV-infected cells [3,14–19]. For instance, LANA stimulates the replication of plasmids with KSHV terminal repeats containing an origin of replication (oriP) as an episome in dividing cells, and maintains these plasmids for at least several months. For these activities, LANA tethers the viral episomes to host chromosomes [14,19]. Several other activities of LANA have been revealed. For example, LANA modulates the transcription of several cellular and viral genes including its own one [17,20–23], and together with activated Ras oncoproteins, it transforms primary rat embryonic fibroblasts *in vitro*. LANA inhibits apoptosis induced by p53 tumor suppressor [20]. However, the precise involvement of these multiple activities in persistent KSHV infection remains to be elucidated.

To further understand the roles of the multifunctional LANA protein in persistent infection, in this study, we surveyed the cellular factors that interact with LANA using yeast two-hybrid screening. One of such proteins was the human myeloid cell nuclear differentiation antigen (MNDA) [24]. MNDA is a nuclear protein with 200-amino acid conserved among the related family (*h*ematopoietic *i*nterferon-inducible *n*uclear proteins with a *200*-amino-acid repeat; HIN-200) members, and is expressed selectively in hematopoietic cells and inducible by interferon (IFN) [25,26]. LANA interacted with MNDA in a human embryonic kidney cell line 293T. Moreover, IFNα induced MNDA in three PEL cell lines, and LANA and MNDA co-localized in a KSHV infected cell line expressing MNDA. We discuss the roles of LANA and MNDA in the context of host-defense mechanism against KSHV.

Materials and Methods

Construction of Plasmids

The L54 phage, supplied from NIH AIDS Research & Reference Reagent Program, includes a part of the KSHV genome that contains the *lana* gene. Using this L54 DNA as a template, the full-length *lana* DNA was amplified by polymerase chain reaction (PCR). The PCR primers used were 5′-TTGATATCAGAATTCATGGCGCCCCCGGGAATGCGCC-3′ and 5′-CATCGAGCTAGCTGCAGTTATGTCATTTCCTGTGGAGAGTC-3′. The DNA polymerase used was KOD dash (TOYOBO, Osaka, Japan). The PCR condition was 1 cycle of 95°C for 1 min, 35 cycles of 95°C for 45 s, 65°C for 10 s and 74°C for 3 min, and 1 cycle of 74°C for 10 min. The amplified *lana* DNA fragment was introduced into pGEM-T vector (Promega, Madison, WI), and the cloned DNA was confirmed by DNA sequencing. To construct a yeast expression plasmid encoding a fusion protein of LANA with a DNA binding domain of the yeast transcription factor GAL4 (pGBKT7/lana), the *lana* DNA in pGEM-T (pGEM-T/lana) was digested with *Eco*RI, and then the isolated fragment was inserted in the pGBKT7 yeast expression vector (Clontech, Palo Alto, CA) in frame to a GAL4 DNA-binding domain (GAL4BD). To construct the full-length *lana* gene fused with a c-Myc epitope (pCMV-Myc/lana), the *lana* fragment isolated from the pGBKT7/lana plasmid by digestion with *Sfi*I and *Xho*I, was introduced into pCMV-Myc mammalian expression vector (Clontech) in frame to a c-Myc epitope. The pSG/H1-LANA(22–1162) is an expression plasmid encoding a fusion protein of LANA(amino acid 22–1162) with the full-length histone H1 as described [19]. The pSG/H1-LANA(275–1162) and pSG/H1-LANA(496–1162) plasmids are derivatives of pSG/H1-LANA(22–1162), and they contain *lana(275–1162)* and *lana(496–1162)* genes in frame to histone H1, respectively. The plasmid pSG5LANA is an expression plasmid for full-length LANA under the control of the simian virus 40 early promoter and was kindly provided by Kenneth Kave (Department of Medicine, Harvard Medical School) [14]. The pACT2 plasmid (Clontech) was used as a yeast expression plasmid encoding a GAL4 activation domain (GAL4AD) fused with a cDNA library. To construct the *MNDA(112–286)* gene fused with a hemaggulutinin (HA) epitope [pCMV-HA/MNDA(112–286)], the pACT2/MNDA(112–286) plasmid isolated from the two-hybrid screening described below was digested with *Sfi*I and *Xho*I, and the *MNDA(112–286)* fragment was introduced into the pCMV-HA mammalian expression vector (Clontech) in frame to a HA epitope. The

pCMV-HA/MNDA(112–245) and pCMV-HA/MNDA(112–235) are derivatives of pCMV-HA/MNDA(112–286). The *MNDA(112–245)* and *MNDA(112–235)* genes were created by PCR with pCMV-HA/MNDA(112–286) as a template. The primers used for the PCR were 5′-CCGGGGATCCGAATTCGCGG-3′, 5′-TATCTCGAGCTAAGTCTTACTGGCCACTGTAGC-3′ for *MNDA(112–245)* and 5′-AAAGAGCTCCTATGTGCTTTTCCCATTTTCTGG-3′ for *MNDA(112–235)*. The DNA polymerase used was PfuTurbo (Stratagene, La Jolla, CA). The PCR condition was 1 cycle of 95°C for 1 min, 25 cycles of 95°C for 1 min, 62°C for 1 min and 72°C for 1 min, and 1 cycle of 72°C for 10 min. The amplified *MNDA* mutant fragments were introduced into pPCR-Script Amp SK (+) vector (Stratagene) and were confirmed by DNA sequencing. The fragments were then introduced into the pCMV-HA vector. To construct mammalian expression plasmids for full-length MNDA [pcDNA3/MNDA(full) and pcDNA3.1/Zeo/MNDA(full)], the full-length *MNDA* gene was inserted into the mammalian expression vectors pcDNA3 (Invitrogen, Carlsbad, CA) and pcDNA3.1/Zeo(+) (Invitrogen), respectively. The pcDNA3.1/Zeo(+) plasmid contains the Zeocin (Invitrogen) resistance gene as a selection marker in mammalian cells. The full-length *MNDA* gene was kindly provided from Dr. Robert C. Briggs (Department of Pathology, Vanderbilt University School of Medicine, Nashville, TN).

Cell Culture

BCBL-1, BC-1, and BC-3 are KSHV-infected B-cell lines, and are derived from PEL [27–29]. U937 is a human promonocytic cell line. These hematopoietic cell lines were cultured in RPMI-1640 (Sigma, St. Louis, MO) supplemented with penicillin (500 U/ml), streptomycin (500 U/ml) and either 10% or 20% fetal bovine serum (FBS). BC-1 and BC-3 cells were kindly provide by Dr. Keiji Ueda (Department of Microbiology, Osaka University School of Medicine, Osaka, Japan). 293T is a human embryonic kidney cell line, and the cells were cultured in Dulbecco's modified Eagle's medium (Sigma) supplemented with 10% FBS, penicillin (500 U/ml) and streptomycin (500 U/ml). All these cell lines were cultured in a 37°C incubator under 5% CO_2. To establish the BCBL-1 cells expressing MNDA protein (BCBL-1/MNDA) and control cells (BCBL-1/Vec), BCBL-1 cells were transfected either with pcDNA3.1/Zeo/MNDA(full) or pcDNA3.1/Zeo(+) by the electroporation method, and the cells were cultured in the presence of Zeocin (200 μg/ml).

To examine the growth property of BCBL-1 cells in the presence of IFNα, the cells (1×10^6) were cultured in 6 cm culture dish containing 4 ml of RPMI-1640/10% FBS with or without recombinant IFNα (6×10^3 U/ml; Peprotech, London, UK). The number of live cells was counted by the trypan blue staining at indicated time points. The cell growth properties of BCBL-1/MNDA and BCBL-1/Vec cells in the presence of IFNα were examined under the same conditions described above, except for culture in a medium containing Zeocin (200 μg/ml).

Yeast Two-Hybrid Screening

The two-hybrid screening was performed using the MATCHMAKER Two-Hybrid System 3 according to the manufacturer's instructions (Clontech). The pACT2 cDNA library used was generated from 550 pooled normal Caucasians (both males and females) peripheral blood leukocytes without human immunodeficiency virus type 1 and hepatitis B virus infection, and the library size was 3.5×10^6 (Clontech). The pGBKT7/lana plasmid and pACT2 cDNA library were transfected into the *Saccharomyces cerevisiae* AH109 reporter strain by the lithium acetate method. The AH109 yeast strain possesses the *HIS3*, *ADE2*, and *MEL1* reporter genes. The *HIS3* and *ADE2* genes encode enzymes that catalyze a step biosynthesizing histidine and adenine, respectively. The *MEL1* gene encodes α-galactosidase and is employed for blue/white screening with X-α-Gal reagents (Clontech). These reporter genes are under the control of GAL4-responsive enhancer element. To examine the *HIS3* and *ADE2* phenotypes, the AH109 transfected with the plasmids was cultured on selection plates containing the minimal synthetic dropout medium containing a nitrogen base, a carbon source, amino acids and nucleosides without histidine, adenine, leucine, and tryptophan. The ability to grow in the medium without leucine and tryptophan was provided by a prey vector (pACT2) and a bait vector (pGBKT7), respectively. To minimize the false positive rate, the selection medium contained 12.5 mM 3-amino-1,2,4-triazole, which is a competitive inhibitor for the enzyme encoded by the *HIS3* gene. The AH109 cells

transfected with the plasmids were cultured on the selection plates at 30°C for 5–10 days. The colonies were picked up and reseeded on the new selection plates. The selections on the plates were repeated three times. The selected clones were then seeded on the selection plates containing X-α-Gal, and the blue colonies were selected as the positive one. From the positive colonies, the plasmids were extracted with the glass beads method (Sigma). The extracted plasmids were transformed into *Escherichia coli* HB101 Electro-Cells (Takara, Tokyo, Japan) by electroporation, and plated on ampicillin plates. The plasmids were then extracted from the *E. coli* HB101 colonies, and the cDNA inserts were characterized by DNA sequencing with an ALF DNA sequencer (Amersham Pharmacia Biotech, Uppsala, Sweden). To check the specificity of interaction between LANA and a partial MNDA, the pGBKT7/lana or pACT2/MNDA(112–286) plasmids were transfected into AH109, and then the yeast was seeded onto selection plates containing X-α-Gal. For control, pGBKT7/lana, pACT2/MNDA(112–286) or each empty vector was co-transformed into AH109, and then the yeast was seeded onto control plates, to which histidine and adenine were added to selection medium. Plasmids encoding a GAL4BD fusion protein of p53 and a GAL4AD fusion protein of simian virus 40 large T-antigen were used as a positive control for the interaction in yeast [30,31].

Immunoprecipitation

The 293T cells (2×10^6) were cultured on 10 cm culture dishes overnight. The cells were then transfected with pCMV-Myc/lana together with pCMV-HA/MNDA(112–286) or pcDNA3/MNDA(full), or the respective control vectors using the lipofection method with FuGENE 6 reagent (Roche, Indianapolis, IN). At two days after transfection, the cells were lysed with 1 ml of the lysis buffer (1.0% Triton X-100, 150 mM NaCl, 50 mM Tris/HCl [pH 8.0], 2 mM PMSF, 1 mM sodium orthovanadate, 1 μg/ml aprotinin in phosphate buffered saline [PBS]) at 4°C for 20 min, and they were then centrifuged at 20,400 × *g* at 4°C for 30 min. These cell extracts were incubated with anti-c-Myc monoclonal antibody-agarose beads (clone 9E10; Clontech) at 4°C overnight with rotation. The beads were then washed with PBS three times and centrifuged. The washed beads were treated with the 2× SDS-PAGE sample buffer (4.0% Sodium dodecyl sulfate (SDS), 20% glycerol, 120 mM Tris/HCl [pH 6.8], 1.44 M 2-mercaptoethanol and 0.02% bromophenol blue) [32], heated at 95°C for 5 min. The proteins in these lysates were separated by electrophoresis on 6% or 10% SDS-polyacrylamide gel (SDS-PAGE). The separated proteins were electronically transferred onto a polyvinylidene difluoride membrane Hybond-P (Amersham Pharmacia Biotech) using a wet method for LANA protein or a semi-dry method for MNDA protein. The membranes were then incubated with Block Ace (Dai-Nippon seiyaku, Osaka, Japan) at room temperature for 1 h with shaking to reduce nonspecific binding of antibodies, and further incubated with rat anti-LANA monoclonal antibody (1/500 dilution; Advanced Biotechnologies Inc., Columbia, MD) or rabbit anti-human MNDA polyclonal antibody (1/1,000 dilution; Calbiochem, La Jolla, CA) at 4°C for overnight. After washing with TBS-T buffer (10 mM Tris/HCl [pH 8.0], 150 mM NaCl, and 0.05% Tween-20), the membrane were further incubated with goat peroxidase-conjugated anti-rat IgG (1/10,000 dilution; Cappel, Costa Mesa, CA) or donkey peroxidase-conjugated anti-rabbit IgG (1/10,000 dilution; Chemicon, Temecula, CA) at room temperature for 1 h with shaking. The membranes were again washed with TBS-T buffer and the antibody binding on the membranes was visualized using ECL Plus Western Blotting Detection System (Amersham Pharmacia Biotech). The molecular weight maker used was precision protein standards (Bio-Rad, Hercules, CA). The procedure for immunoprecipitation with anti-MNDA antibody was carried out with some modifications. The cell extracts prepared from 293T cells transfected with either pCMV-Myc/lana, pSG5LANA, pSG/H1-LANA(22–1162), pSG/H1-LANA(275–1162) or pSG/H1-LANA(496–1162) together with either pCMV-HA/MNDA(112–286), pCMV-HA/MNDA(112–245), pCMV-HA/MNDA (112–235) or pcDNA3/MNDA(1–407), or the respective control vectors as described, were incubated with protein G-Sepharose (Zymed, San Francisco, CA) at 4°C for 1 h with rotation to remove nonspecific binding. The pre-cleared extracts were then incubated overnight with mouse anti-HA monoclonal antibody (clone HA-7; Sigma) at 4°C with rotation, further incubated with protein G-Sepharose at 4°C for 1 h with rotation. The sepharose was washed with PBS three times and centrifuged. The sepharose was treated with the 2× SDS-PAGE sample buffer and

heated at 95°C for 5 min. The lysates were used for Western blot analysis as described above.

RT-PCR

Total RNAs were isolated from KSHV-infected PEL cell lines, BCBL-1, BC-1, and BC-3, with Isogen (Nippon gene, Toyama, Japan) according to the manufacturer's instructions. The RT-PCR analysis for *MNDA* transcript was performed using 2 μg of total RNA and Ready-To-Go RT-PCR Beads (Amersham Pharmacia Biotech). A oligo d(T) primer was used for the reverse transcription step, and the condition was 42°C for 30 min and 95°C for 5 min. The *MNDA* 5′ and *MNDA* 3′ specific primers used for the PCR step were 5′-TGCTACAGTGGCCAGTAAGA-3′ and 5′-TGACCTTGATGAAGCTGTGA-3′, respectively, and the condition was 94°C for 2 min, 50 cycles of 94°C for 30 s, 50°C for 30 s and 72°C for 1 min, and 1 cycle of 72°C for 7 min. The amplified products were confirmed as a *MNDA* fragment (470 bp) by DNA sequencing. The β-actin specific primers were supplied from Promega (Madison, WI). The RT-PCR condition was 42°C for 30 min and 95°C for 5 min for RT, and 1 cycle of 94°C for 2 min, 25 cycles of 94°C for 30 s, 65°C for 1 min, 68°C for 2 min, and 1 cycle of 68°C for 7 min for PCR. The RT-PCR was carried out using a GeneAmp PCR system 9700 (Applied Biosystems, Foster City, CA).

Indirect Immunofluorescence Assay

The BCBL-1/MNDA and BCBL-1/Vec cells were dispersed on slide glasses, dry by air-blow and fixed with 100% methanol at −20°C for 5 min. The fixed cells were incubated with rat anti-LANA monoclonal antibody (1/100 dilution) and rabbit anti-human MNDA polyclonal antibody (1/100 dilution) in PBS including 10% Block Ace at 37°C for 1 h. The cells on the slides were washed with PBS for 5 min at room temperature three times and incubated with goat rhodamine (Rhod)-conjugated anti-rat IgG (1/1,000 dilution; Cappel) and goat fluorescein isothiocyanate (FITC)-conjugated anti-rabbit IgG (1/1,000 dilution; Immunotech, Marseille, France) in PBS including 10% Block Ace at 37°C for 1 h. The stained cells were visualized with a confocal laser scanning microscope MRC-1024ES and software the LaserSharp (Bio-Rad).

Results

Identification of Myeloid Cell Nuclear Differentiation Antigen as a LANA Interaction Protein

To identify cellular proteins that interact with KSHV LANA, a human leukocyte cDNA library fused with the activation domain of GAL4 (GAL4AD-cDNA) was screened by the yeast two-hybrid method with a full-length LANA fused with the DNA binding domain of GAL4 (GAL4BD-LANA). We obtained 26 positive yeast transformants from 1.26×10^7 independent clones. The plasmids were prepared from these 26 transformants, and their cDNA fragments were characterized by DNA sequencing. BLAST sequence similarity search revealed that 2 of these 26 cDNAs encoded same part of *MNDA* gene. MNDA is a member of HIN-200 family. HIN-200 family has one or two 200-amino acid length motif conserved among the family members, and the expression is hematopoietic-specific and inducible by IFN. The full-length *MNDA* gene consists of 407 amino acids, and the isolated *MNDA(112–286)* gene contained a basic amino acid region, a nuclear localization signal and half of the 200-amino acid motif.

To confirm the interaction of LANA with the isolated partial MNDA in yeast, the AH109 yeast strain used for the two-hybrid assay was re-transformed with the isolated GAL4AD-MNDA plasmid and the GAL4BD-LANA plasmid. The transformed yeasts grew on media lacking adenine and histidine (Fig. 1,

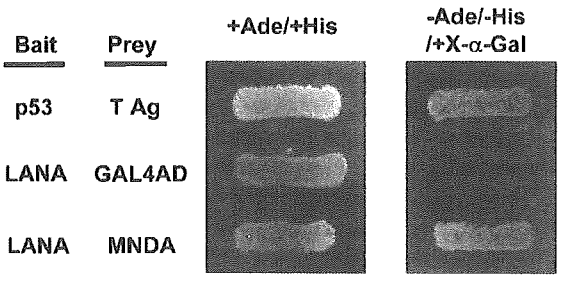

Fig. 1. Interaction of LANA with a partial MNDA in yeast: The bait plasmids encoding GAL4BD-p53 or GAL4BD-LANA, and the prey plasmids encoding GAL4AD-T-antigen, GAL4AD or GAL4AD-MNDA, were co-transfected into a yeast AH109 reporter strain. The yeasts were then cultured on the plate with adenine and histidine (left panel) or the selection plate free of adenine and histidine with X-α-Gal reagents (right panel). The GAL4BD-p53 and GAL4AD-T-antigen were used as positive control [31,32].

right panel), and exhibited a blue color in the presence of X-α-Gal, the phenotype mediated by α-galactosidase. The AH109 yeast strain possesses the *HIS3*, *ADE2*, and *MEL1* reporter genes. These reporter genes are under the control of GAL4-responsive upstream element. In contrast, the yeasts transformed by the GAL4BD-LANA together with the plasmid encoding the GAL4AD without a cDNA or those transformed by the GAL4AD-MNDA plasmid together with the plasmid encoding GAL4BD without *lana* gene failed to grow on the selection media (Fig. 1, right panel, data not shown), but grew in media containing adenine and histidine. Considered together, these results indicated that full-length LANA interacted with a part of MNDA protein (112–286 amino acids) in yeast.

Interaction of LANA with MNDA in Mammalian Cells

To examine the interaction of LANA with MNDA in mammalian cells, we constructed the *lana* and *MNDA(112–286)* genes with the distinct epitope tags. The *HA-MNDA(112–286)* gene has a HA epitope at the N-terminus of MNDA(112–286), while the *Myc-LANA* gene has a c-Myc epitope at the N-terminus of the full-length LANA. The HA-MNDA plasmid together either with the Myc-LANA or the control plasmid encoding the c-Myc epitope (Myc-Epitope) were transfected into a human embryonic kidney cell line 293T using a lipofection method. At 48 h after transfection, the cell lysates were prepared, and immunoprecipitated with an anti-Myc antibody. Western blot analysis using anti-MNDA antibody detected the HA-MNDA(112–286) protein in the Myc-LANA immunoprecipitate, but not in the Myc-Epitope one (Fig. 2A). This was not due to the reduced expression of HA-MNDA(112–286) in 293T cells transfected with the Myc-Epitope plasmid, since an equivalent amount of HA-MNDA(112–286) protein was expressed in the 293T cells transfected with the Myc-Epitope plasmid and those with the Myc-LANA plasmid. Conversely, the LANA protein was detected in the anti-HA antibody immune-complex prepared from 293T cells transfected with the Myc-LANA plasmid together with HA-MNDA(112–286) plasmid, but not in those transfected with Myc-LANA without HA-MNDA(112–286) (Fig. 2B). We also examined whether LANA precipitates a full-length MNDA without the epitope tag. As shown in Fig. 2(C), the MNDA protein was precipitated with Myc-LANA by anti-Myc antibody from 293T cells transfected with these two plasmids, whereas it was not with Myc epitope protein. In the reverse experiment, the Myc-LANA protein was precipitated with the full-length MNDA by anti-MNDA antibody (data not shown). Considered together, these results showed that full-length LANA interacts with full-length MNDA in 293T cells.

To further delineate the regions responsible for the interaction, three LANA mutant plasmids and two MNDA ones were constructed (Fig. 3). Cell extracts were prepared from 293T transfected with the LANA mutant plasmids together with the indicated HA-MNDA(112–286) one. The extracts were then immunoprecipitated with anti-HA antibody, and the LANA protein in the immunoprecipitate was analyzed by Western blotting analysis. Anti-LANA antibody detected wild-type LANA(1–1162) and H1-LANA(22–1162) only together with MNDA (112–286), whereas the antibody did not detect H1-LANA(275–1162) or H1-LANA(496–1162), indicating that the amino acid 22–274 of LANA is required for the interaction with MNDA (Fig. 3B). Conversely, the LANA protein was detected in the HA-MNDA(112–286) complex immunoprecipitated with anti-HA antibody, but not in the HA-MNDA (112–245) and the HA-MNDA(112–235) one (Fig. 3C). Thus, these results indicated that the amino acid 245–286 of MNDA is required for the interaction with LANA.

Induction of MNDA Transcript by IFNα

The *MNDA* is expressed in several hematopoietic cell lines [25,26] and it is induced by IFNα. Thus, we next investigated the *MNDA* expression in three KSHV-infected PEL cell lines. The *MNDA* transcript was detected in U937 cells with RT-PCR analysis, whereas it was not in BCBL-1 cells (Fig. 4A). The *MNDA* transcript was, however, detected in BCBL-1 cells 3 h after treatment with IFNα (3×10^3 U/ml), and the expression continued till 48 h (data not shown), with the peak expression at 6 h after the treatment (Fig. 4(A)), although the level of the expression was less than that in U937 cells. DNA sequencing analysis confirmed that the RT-PCR product was derived from the *MNDA* transcript. In addition, *MNDA* transcript was undetectable in two other PEL cell lines, BC-1

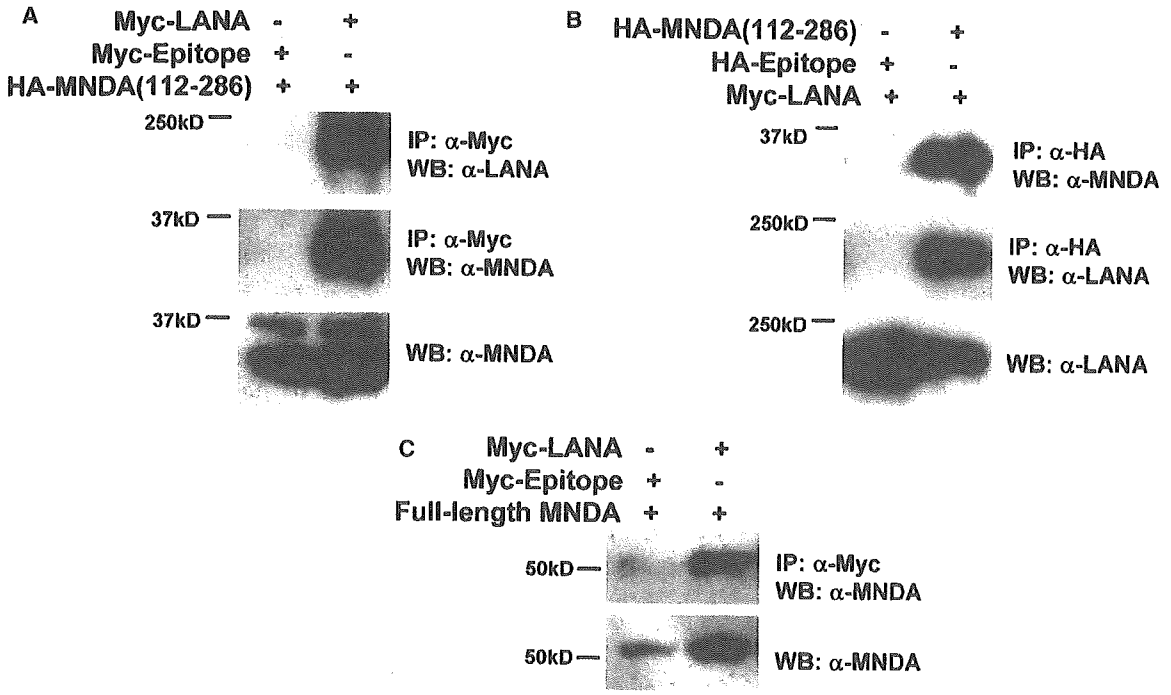

Fig. 2. Interaction of LANA with MNDA in 293T cells: (A) The 293T cells were transfected with the HA-MNDA(112–286) plasmid together with either the Myc-LANA or the Myc-Epitope one. At 48 h after transfection, the cell extracts were prepared, and immunoprecipitated with anti-c-Myc antibody-agarose beads. The proteins in the immunoprecipitate were characterized by Western blot analysis using anti-LANA antibody (upper panel) or anti-MNDA antibody (middle panel). The cell extracts described above were also characterized by Western blot analysis with anti-MNDA antibody without immunoprecipitation (lower panel). The expected molecular weight of the HA-MNDA(112–286) protein is 20.4 kDa and the reported LANA protein is about 220 kDa. (B) 293T cells were transfected with the Myc-LANA plasmid together with either the HA-MNDA (112–286) or the HA-Epitope one. At 48 h after transfection, their cell extracts were incubated with anti-HA antibody. The immunoprecipitate with anti-HA antibody was characterized by Western blot analysis using anti-MNDA antibody (upper panel) or anti-LANA antibody (middle panel). The cell extracts described above were also characterized by Western blot analysis with anti-LANA antibody without immunoprecipitation (lower panel). (C) 293T cells were transfected with the full-length MNDA plasmid together either with the Myc-LANA or the Myc-Epitope one. At 48 h after transfection, their cell extracts were incubated with anti-c-Myc antibody-agarose beads. The immunoprecipitate was characterized by Western blot analysis using anti-MNDA antibody (upper panel) or anti-HA antibody (middle panel). The molecular weight of the full-length MNDA protein is 55 kDa. The experiments described above were repeated three times to confirm reproducibility. The positions of the molecular weight standard proteins are indicated.

and BC-3, and it was induced by IFNα (Fig. 4B). We could not, however, detect the MNDA protein in BCBL-1 cells treated with IFNα by Western blot analysis (data not shown). These results showed that the *MNDA* transcript was inducible by IFNα in all the three KSHV-infected cell lines.

Subcellular Localization of LANA and MNDA

To further confirm the physical interaction of LANA with MNDA in PEL cell lines, we investigated the subcellular localization of LANA and MNDA in BCBL-1 cells. An indirect immunofluorescence assay using anti-LANA antibody detected the punctate expression of LANA in the nuclei of BCBL-1 cells (Fig. 5A), as reported previously [14]. On the other hand, specific staining with anti-MNDA antibody was observed in U937 cells (Fig. 5A). We established a BCBL-1 cell line expressing stably the MNDA protein by plasmid transfection. Western blot analysis detected the MNDA protein in BCBL-1 cells transfected with the MNDA plasmid (BCBL-1/MNDA) but not in cells transfected with the vector plasmid (BCBL-1/Vec) (Fig. 5B). In this BCBL-1/MNDA cell, anti-MNDA antibody detected a sand-like expression (Fig. 5C). This is specific to MNDA

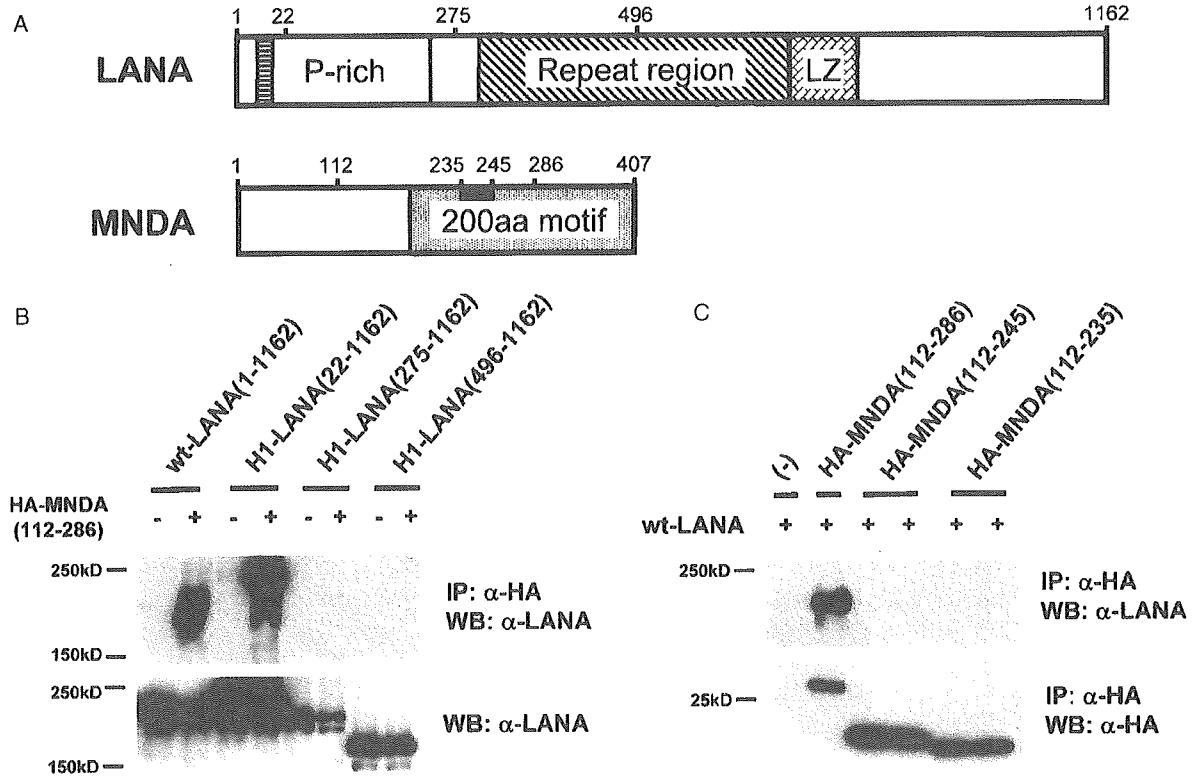

Fig. 3. The regions of LANA and MNDA required for their interaction: (A) Schematic structural representation of LANA and MNDA. Proline-rich region (P-rich). acidic repeat (Repeat region), putative leucine-zipper (LZ) and chromosome binding site (horizontal stripe) of LANA, and 200 amino acid motif (200aa motif) and MFHATVA sequence (black box) of MNDA are indicated. (B) The 293T cells were transfected with the HA-MNDA(112–286) plasmid together either with the wild-type LANA(1–1162), the H1-LANA(22–1162), the H1-LANA(275–1162) or the H1-LANA(496–1162) one. At 48 h after transfection, the cell extracts were prepared, and immunoprecipitated with anti-HA antibody. The proteins in the immunoprecipitate were characterized by Western blot analysis using anti-LANA antibody (upper panel). The cell extracts described above were also characterized by Western blot analysis with anti-LANA antibody without immunoprecipitation (lower panel). (C) The 293T cells were transfected with the wild-type LANA(1–1162) plasmid together either with the HA-MNDA(112–286), the HA-MNDA(112–245) or the HA-MNDA(112–235) one. At 48 h after transfection, the cell extracts were prepared, and immunoprecipitated with anti-HA antibody. The proteins in the immunoprecipitates were characterized by Western blot analysis using anti-LANA antibody (upper panel) or with anti-HA antibody (lower panel).

protein, since the same antibody did not detect the signal above the background level in BCBL-1/Vec cells, and this staining pattern was similar to that in U937 cells that constitutively express endogenous MNDA protein (Fig. 5A). The anti-LANA antibody detected the punctate expression of LANA in the nuclei of BCBL-1/MNDA cells, similar to parental BCBL-1 cells (Fig. 5C, lower left panel), and double staining showed that LANA protein co-localized in part with MNDA in BCBL-1/MNDA cells. These results indicated that a part of LANA proteins co-localizes with MNDA in BCBL-1 cells expressing a high amount of MNDA.

MNDA did not Affect Cell Growth of BCBL-1 Cells

IFNα reportedly inhibits proliferation of KSHV-infected cell lines [33]. Since many of IFNα activities are mediated by IFN-inducible genes, we investigated whether MNDA inhibits proliferation of KSHV-infected cells. As shown in Fig. 5, IFNα inhibited the cell growth of BCBL-1 as reported previously [33], while the cell growth of BCBL-1/MNDA was similar to that of BCBL-1/Vec cells. These results suggested that MNDA does not mediate IFNα-induced growth inhibition of KSHV-infected cells.

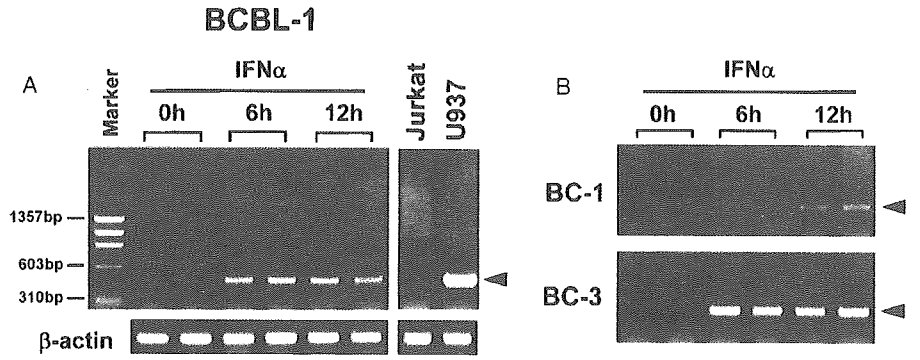

Fig. 4. IFNα-induced expression of *MNDA* transcript in KSHV-infected cell lines (A, B) Total RNAs were isolated from BCBL-1, BC-1, or BC-3 cell lines at the indicated times after IFNα treatment or from Jurkat or U937 cell lines without IFNα treatment. The RT-PCR products amplified from the isolated total RNAs were size-separated on 1% agarose gel, and stained with ethidium bromide. The molecular weight marker was *ϕX*174 DNA digested with *Hae*III. The amplified product from the *β-actin* transcript indicates the similar amount of RNA used for the RT-PCR assay. Experiments were curried out in duplicate, and repeated three times to confirm the reproducibility. Arrowhead indicates the specific product from *MNDA* transcript.

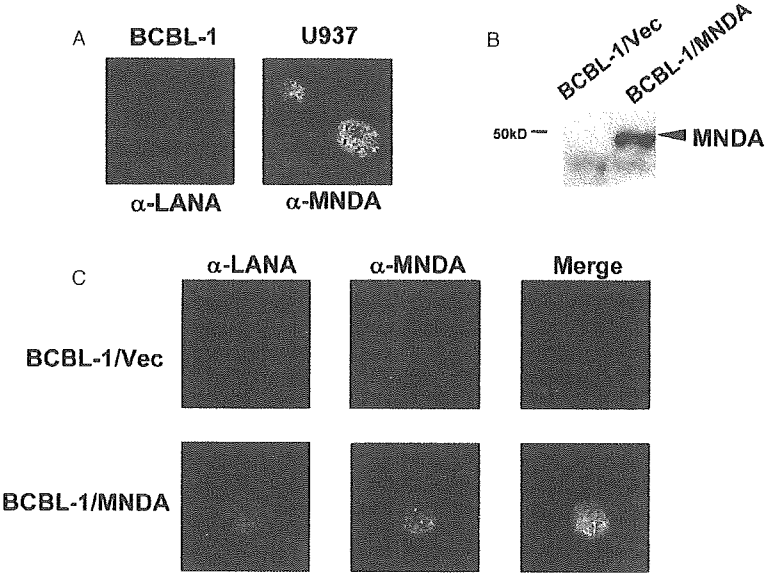

Fig. 5. Subcellular localizations of LANA and MNDA in BCBL-1 cells: (A) BCBL-1 and U937 cells on a glass slide were fixed with 100% methanol at −20°C for 5 min and then incubated with rat anti-LANA antibody (1/100 dilution) and rabbit anti-MNDA antibody (1/100 dilution). After washing, the cells were incubated with Rhod-conjugated anti-rat IgG (1/1,000 dilution) and FITC-conjugated anti-rabbit IgG (1/1,000 dilution), respectively. The stained cells were examined under confocal laser scanning microscopy (magnification, ×1,200). (B) Cell extracts were prepared from BCBL-1/MNDA and BCBL-1/Vec cells, and the amount of MNDA protein in the extracts was measured by Western blot analysis using an anti-MNDA antibody. Arrowhead indicates the specific band corresponding to the full-length MNDA (55 kDa). (C) BCBL-1/MNDA and BCBL-1/Vec cells on a glass slide were fixed with 100% methanol at −20°C for 5 min and then incubated with rat anti-LANA antibody and anti-MNDA antibody. After washing, the cells were further incubated with Rhod-conjugated anti-rat IgG and FITC-conjugated anti-rabbit IgG. The stained cells were examined under confocal laser scanning microscope (magnification, ×1,200).

Discussion

By using yeast two-hybrid screening, we isolated MNDA as a LANA interaction protein. LANA interacted with MNDA in a 293T cell line, and co-localized with MNDA in KSHV-infected cells expressing *MNDA*. Moreover, IFNα induced the expression of MNDA in three KSHV infected cell

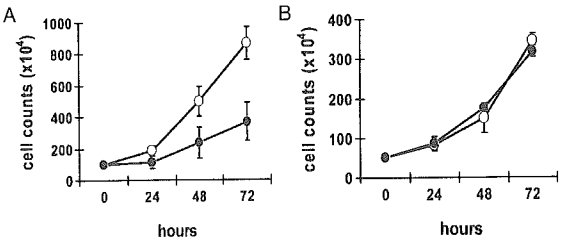

Fig. 6. Effects of MNDA and IFNα on the cell growth of BCBL-1: (A) One million BCBL-1 cells were cultured in 6 cm culture dishes containing 4 ml of RPMI1640/10% FCS with (closed circles) or without (open circles) recombinant IFNα (6×10^3 U/μl). The number of live cells was determined by the trypan blue staining at the indicated time points. The presented data are mean ± SD of three experiments. (B) Half million of BCBL-1/MNDA (open circles) and BCBL-1/Vec cells (closed circles) were cultured in 6 cm culture dish containing 4 ml of RPMI1640/10% FCS containing Zeocin (200 μg/ml). The number of live cells was examined by trypan blue staining at the indicated time points. Representative data are shown here; experiments were carried out in duplicate, and repeated three times.

lines. Since IFN-inducible genes mediate many of IFN-mediated host-defense activities against various viruses, the present results suggest that LANA attenuates the host defense mechanism against KSHV triggered by IFNα.

MNDA belongs to a family of homologous proteins known as the HIN-200 family, each containing at least one 200-amino acid repeat [25,26]. The list contains the human IFI16, AIM 2, MNDA, and the murine p202, p203, p204, and D3 proteins. The isolated MNDA(112–286) as a LANA interaction protein contained half of the 200-amino acid motif with an identical sequence (MFHATVA) conserved among all family members. Unlike MNDA(112–286), MNDA (112–245), and MNDA(112–235) did not interact with LANA in 293T cells (Fig. 3) MNDA(112–235) does not have the MFHATVA motif. Although MNDA(112–245) has the MFHATVA motif but it has the further deletion of the 200-amino acid motif relative to MNDA(112–286). These results suggest that the 200-amino acid motif of MNDA is involved in the interaction with LANA, and LANA binds to other HIN-200 family members.

One of the IFN actions against the virus is the growth inhibition of virus-infected cells [34]. Indeed, IFNα has been shown to inhibit the cell growth of KSHV-infected cell lines [33]. The present results, however, showed that the exogenous expression of MNDA did not affect the cell growth of BCBL-1 cell line infected with KSHV. These results suggest that the induction of MNDA alone is not sufficient for IFNα-induced growth inhibition of KSHV-infected cells. Since IFN has a number of activities to virus-infected cells, these results may indicate that MNDA is involved in other aspects of IFN actions against HHV-8-infected cells.

The present results did not clarify how the interaction of LANA with MNDA modulates IFN activities, partly because the physiological function(s) of MNDA has not been elucidated yet. Several HIN-200 family members have been shown to regulate the transcription of cellular genes. MNDA also induces the expression of a cellular *Dlk1* gene in human K562 myeloid cell line, the product of which is essential for normal hematopoiesis [35]. On the other hand, LANA represses or activates transcription from some promoters [12,36,37]. LANA mutants suggested that the N-terminal amino acid 22–274 of LANA is required for the interaction with MNDA. This region of LANA has been shown to be involved in the transcriptional repression [36]. Thus, LANA may modulate the transcriptional regulation by the binding to MNDA. Further analysis is required to elucidate the role of HIN-200 family members and their interaction with LANA in the host defense mechanism against KSHV.

Acknowledgments

We thank Dr. Robert C. Briggs for providing the full-length *MNDA* gene, Dr. Kenneth Kaye for providing LANA expression vector, Dr. Keiji Ueda for providing BC-1 and BC-3 cells, and Dr. Eishin Yaoita for help with confocal laser scanning microscope. We also thank Ryoko Fujita for the excellent technical assistance.

This work was supported in part by Grant-in-Aid for Scientific Research from the Ministry of Education, Culture, Sports, Science and Technology of Japan, Grant-in-Aid from the Niigata University Science Foundation and Grant for Promotion of Niigata University Research Projects.

References

1. Chang Y., Cesarman E., Pessin M.S., Lee F., Culpepper J., Knowles D.M., and Moore P.S., Science *266*, 1865–1869, 1994.
2. Moore P.S. and Chang Y., N Engl J Med *332*, 1181–1185, 1995.

3. Cesarman E., Chang Y., Moore P.S., Said J.W., and Knowles D.M., N Engl J Med *332*, 1186–1191, 1995.
4. Cesarman E., Moore P.S., Rao P.H., Inghirami G., Knowles D.M., and Chang Y., Blood *86*, 2708–2714, 1995.
5. Soulier J., Grollet L., Oksenhendler E., Cacoub P., Cazals-Hatem D., Babinet P., D'Agay M.F., Clauvel J.P., Raphael M., Degos L., and Sigaux F., Blood *86*, 1276–1280, 1995.
6. Boshoff C., Schulz T.F., Kennedy M.M., Graham A.K., Fisher C., Thomas A., McGee J.O., Weiss R.A., and O'Leary J.J., Nat Med *1*, 1274–1278, 1995.
7. Kedes D.H., Lagunoff M., Renne R., and Ganem D., J Clin Invest *100*, 2606–2610, 1997.
8. Kellam P., Boshoff C., Whitby D., Matthews S., Weiss R.A., and Talbot S.J., J Hum Virol *1*, 19–29, 1997.
9. Rainbow L., Platt G.M., Simpson G.R., Sarid R., Gao S.J., Stoiber H., Herrington C.S., Moore P.S., and Schulz T.F., J Virol *71*, 5915–5921, 1997.
10. Gao S.J., Kingsley L., Li M., Zheng W., Parravicini C., Ziegler J., Newton R., Rinaldo C.R., Saah A., Phair J., Detels R., Chang Y., and Moore P.S., Nat Med *2*, 925–928, 1996.
11. Kedes D.H., Operskalski E., Busch M., Kohn R., Flood J., and Ganem D., Nat Med *2*, 918–924, 1996.
12. Schwam D.R., Luciano R.L., Mahajan S.S., Wong L., and Wilson A.C., J Virol *74*, 8532–8540, 2000.
13. Russo J.J., Bohenzky R.A., Chien M.C., Chen J., Yan M., Maddalena D., Parry J.P., Peruzzi D., Edelman I.S., Chang Y., and Moore P.S., Proc Natl Acad Sci USA *93*, 14862–14867, 1996.
14. Ballestas M.E., Chatis P.A., and Kaye K.M., Science *284*, 641–644, 1999.
15. Ballestas M.E. and Kaye K.M., J Virol *75*, 3250–3258, 2001.
16. Hu J., Garber A.C., and Renne R., J Virol *76*, 11677–11687, 2002.
17. Garber A.C., Shu M.A., Hu J., and Renne R., J Virol *75*, 7882–7892, 2001.
18. Cotter M.A. 2nd and Robertson E.S., Virology *264*, 254–264, 1999.
19. Shinohara H., Fukushi M., Higuchi M., Oie M., Hoshi O., Ushiki T., Hayashi J., and Fujii M., J Virol *76*, 12917–12924, 2002.
20. Friborg J., Kong W., Hottiger M.O., and Nabel G.J., Nature *402*, 889–894, 1999.
21. Garber A.C., Hu J., and Renne R., J Biol Chem *277*, 27401–27411, 2002.
22. Sarid R., Wiezorek J.S., Moore P.S., and Chang Y., J Virol *73*, 1438–1446, 1999.
23. Jenner R.G. and Boshoff C., Biochim Biophys Acta *1602*, 1–22, 2002.
24. Hudson C.R., Bellew T., Briggs J.A., Casey S.B., and Briggs R.C., Hybridoma *7*, 541–553, 1998.
25. Lengyel P., Choubey D., Li S.J., and Datta B., Semin Virol *6*, 203–213, 1995.
26. Johnstone R.W. and Trapani J.A., Mol Cell Biol *19*, 5833–5838, 1999.
27. Renne R., Zhong W., Herndier B., McGrath M., Abbey N., Kedes D., and Ganem D., Nat Med *2*, 342–346, 1996.
28. Miller G., Heston L., Grogan E., Gradoville L., Rigsby M., Sun R., Shedd D., Kushnaryov V.M., Grossberg S., and Chang Y., J Virol *71*, 314–324, 1997.
29. Arvanitakis L., Mesri E.A., Nador R.G., Said J.W., Asch A.S., Knowles D.M., and Cesarman E., Blood *88*, 2648–2654, 1996.
30. Li B. and Fields S., FASEB J *7*, 957–963, 1993.
31. Iwabuchi K., Li B., Bartel P., and Fields S., Oncogene *8*, 1693–1696, 1993.
32. Harlow E. and Lane D., *Using Antibodies*, Cold Spring Harbor Laboratory Press, Cold Spring Harbor, New York, 1999.
33. D'Agostino G., Arico E., Santodonato L., Venditti M., Sestili P., Masuelli L., Coletti A., Modesti A., Picchio G., Mosier D.E., Ferrantini M., and Belardelli F., J Interferon Cytokine Res *19*, 1305–1316, 1999.
34. Knipe D.M. and Howley P.M., *Fields Virology*, Lippincott Williams & Wilkins, Philadelphia, 2001.
35. Doggett K.L., Briggs J.A., Linton M.F., Fazio S., Head D.R., Xie J., Hashimoto Y., Laborda J., and Briggs R.C., J Cell Biochem *86*, 56–66, 2002.
36. Krithivas A., Young D.B., Liao G., Greene D., and Hayward S.D., J Virol *74*, 9637–9645, 2000.
37. Renne R., Barry C., Dittmer D., Compitello N., Brown P.O., and Ganem D., J Virol *75*, 458–468, 2001.

Leukemia & Lymphoma, November 2004 Vol. 45 (11), pp. 2343–2347

Taylor&Francis
healthsciences

Viral Load of Human Herpesvirus 8 (HHV-8) in the Circulatory Blood Cells Correlates with Clinical Progression in a Patient with HHV-8-associated Solid Lymphoma with AIDS-associated Kaposi's Sarcoma

JIAN SONG[a], ATSUSHI YOSHIDA[b], YOSHIHIKO YAMAMOTO[c], HARUTAKA KATANO[d], KEISUKE HAGIHARA[a], SHINICHI OKA[c], SATOSHI KIMURA[b,c] and KAZUYUKI YOSHIZAKI[a,*]

[a]*Department of Medical Science I, School of Health and Sport Sciences, Osaka University, Osaka, Japan;* [b]*Department of Infection Control and Prevention, Graduate School of Medicine, University of Tokyo, Tokyo, Japan;* [c]*AIDS Clinical Center, International Medical Center of Japan, Tokyo, Japan and* [d]*Department of Pathology, National Institute of Infectious Diseases, Tokyo, Japan*

(Received 25 June 2004)

We encountered a case of a rapidly progressive HHV-8-associated solid lymphoma with AIDS-associated Kaposi's sarcoma (KS). HHV-8 DNA load in whole blood cells was analyzed quantitatively by real-time PCR using amplification of the HHV-8-encoded ORF26 gene. Ours is the first observation that the rapid increase in the HHV-8 viral load (from 1.9×10^4 copies/μg to 1.6×10^6 copies/μg in 40 days) in conjunction with low CD4 + cell counts was accompanied by an accelerated clinical disease progression. The results indicate that the quantity of circulating HHV-8 is measurable with real-time PCR and can provide clinically useful information.

Keywords: HHV-8-associated solid lymphoma; HHV-8; Viral load; ORF26; Real-time PCR

INTRODUCTION

Human herpesvirus-8 (HHV-8) is etiologically linked to Kaposi's sarcoma (KS), the most common malignancy in patients with AIDS [1,2]. HHV-8 DNA is consistently found in KS tissues, and is detected in peripheral blood mononuclear cells (PBMC) of human immunodeficiency virus (HIV)-infected individuals [3,4]. Detection of HHV-8 DNA in PBMC from HIV type 1-infected persons is associated with an increased risk of subsequent development of KS [4,5] and with the clinical stage of KS [5,6]. AIDS-associated primary effusion lymphoma (PEL, body-cavity based lymphoma), a distinct subtype of non-Hodgkin's lymphoma (NHL), is another HHV-8-associated neoplasm, which is typically present as a malignant effusion without solid tumor masses in the body cavity of AIDS patients [7]. Recently, solid organ involvement of HHV-8-associated lymphomas has also been reported in some AIDS patients [8–11]. HHV-8-associated solid lymphomas were characterized by expressing CD30, exhibiting anaplastic large cell morphology and carrying clonal immunoglubulin gene rearrangement that indicates B-cell origin despite the usual presence of a non-specific immunophenotype. HHV-8 DNA and latency-associated nuclear antigen (LANA) have been detected in lymphoma cells from HHV-8-associated solid lymphoma patients. Epstein-barr virus (EBV) co-infection was also found in most of these patients. There have been no reports, however, of an elevated HHV-8 DNA load in serum nor in whole blood cells with HHV-8-associated solid lymphoma in AIDS patients. Yamamoto [12] reported a case of rapidly progressive HHV-8-associated solid lymphoma with anaplastic large cell morphology followed by systemic KS, which is complemented by our kinetic study of the HHV-8 DNA load and CD4 + cell counts in blood cells in the same patient. The quantitative real-time PCR (Taqman PCR) technique provides an accurate and reproducible measurement of the level of HHV-8 in the circulatory blood cells. We used this technique to quantify the HHV-8 DNA load in whole blood cells. Ours is the first report of the correlation between a rapid

*Corresponding author. Address: Department of Medical Science I, School of Health and Sport Sciences, Osaka University, 2-1 Yamadaoka, Suita, Osaka, 565-0871, Japan. Tel.: + 81-6-6879-8960. Fax: + 81-6-6879-8971. E-mail: kyoshizaki@hpc.cmc.osaka-u.ac.jp

ISSN 1042-8194 print/ISSN 1029-2403 online
DOI: 10.1080/10428190412331283242

increase of HHV-8 viral load in conjunction with low CD4 + cell counts and disease progression.

CASE REPORT

Patient History

The clinical history, as well as the physical and laboratory findings including treatment modalities of this patient were described previously [12]. The patient was a 30-year-old Caucasian male with homosexual behavior and intravenous drug use history for 10 years. He had a 6-year HIV-1 infection history but did not contract any opportunistic infections until red spots were found on the skin of the arms, chest and abdomen and later on diagnosed as KS. Upon diagnosis with KS, the CD4 + cell count was 75/μl and HIV-1 plasma viral load was 431,992 copies/ml. He was transferred to the AIDS Clinical Center of the International Medical Center of Japan in Tokyo due to loss of consciousness, where Highly Active Antiretroviral Therapy (HAART) was stopped because he was unconscious. KS lesions were observed on his whole body. Liposomal doxorubicin (20 ng/m^2) was administered twice intravenously to treat KS. Whole blood cells were obtained before and after chemotherapy and the purified DNA was used for HHV-8 DNA quantification by means of real-time PCR. Biopsy results from the enlarged axillary and cervical lymph nodes showed large cell lymphoma morphology. HHV-8 and Epstein-Barr virus (EBV) producing proteins were detected in the lymphoma cells. Enzyme immunoassay (EIA) and immunofluorescence assay (IFA) were negative for the serum anti-HHV-8 antibody. The patient died 6 days after the induction of a CHOP regimen [12]. In autopsy, lymphoma cells were found not only in the cervical, mediastinal and inguinal lymph nodes, but also in the spleen, tonsils, gastrointestinal mucosa, lungs, adrenal glands and bone marrow. The lymphoma cells displayed anaplastic large blastic cell morphology and had an undeterminant phenotype. In immunohistochemistry, CD30-positive, CD43-positive, CD45RO-positive, CD45-positive, CD4-negative, CD5-negative, CD8-negative, CD15-negative and CD20-negative were detected in the lymphoma cells. Also, HHV-8-encoded LANA was expressed in most lymphoma cells. EBV-encoded small RNA-1 (EBER-1) was expressed in some lymphoma cells by *in situ* hybridization. KS was found in skin and peri-lymph node soft tissue in the inguinal region.

Establishment of Quantitative Real-time PCR Assay for HHV-8-Encoded ORF26 Gene

The amount of HHV-8 DNA purified from whole blood cells was determined by real-time PCR using amplification of the conserved region of the open reading frame (ORF) 26 gene. The primers and probe of ORF26 were conducted by the method described by White [13]. The amount of human genomic DNA present in the same sample was also determined by real-time PCR using amplification of the human GAPDH (glyceraldehyde-3-phosphate dehydrogenase) gene. The quantification of human GAPDH was used to normalize the target DNA. The primers and probes used to quantify ORF26 and GAPDH are shown in Table I. Quantitative real-time PCR was performed in duplicate with the aid of the Taqman Universal PCR Master Mix kit and the PE Biosystem 5700 sequence detector (Applied Biosystems, Foster City, CA, USA) in accordance with the manufacturer's protocol. Briefly, the reaction volume of 50 μl contained 25 μl of 2 × master buffer, 15 pmoles of 1 of primers, 10 pmoles of the dual-labeled probe, and 0.1 μg DNA of 1 of samples to be tested. All assays showed a linear relationship between the value of threshold cycle (Ct) for standards and the logarithm of the amount of ORF26 DNA added to the reaction. The PCR products were further examined by acrylamide gel electrophoresis for confirmation of specific HHV-8 DNA amplification.

Relationship Analysis of HHV-8 DNA Load, CD4 + cell Counts and Clinical Course

Real-time quantitative PCR of the HHV-8 ORF26 gene showed that the HHV-8 DNA load in whole blood cell was constitutively high (1.9×10^4 copies/μg) at the beginning of anti-KS therapy (Liposomal doxorubicin, 20 mg/m^2) (Fig. 1), while the CD4 + cell count was very low (32/μl) even though the patient had been treated with HAART. Systemic KS treatment with liposomal doxorubicin (20 ng/m^2) was administered twice intravenously

TABLE I Oligonucleotide primers used for real-time PCR assay

Name	Position[a]	Polarity	Sequence[b]
Taq26F	379 – 399	Sense	5'-CTCGAATCCAACGGATTTGAC-3'
Taq26R	434 – 452	Antisense	5'-TGCTGCAGAATAGCGTGCC-3'
Probe26	410 – 429	Sense	5'-**F**-CCATGGTCGTGCCGCAGCA-**T**-3'
GapdhF	6 – 24	Sense	5'-GAAGGTGAAGGTCGGAGTC-3'
GapdhR	212 – 231	Antisense	5'-GAAGATGGTGATGGGATTTC-3'
GapdhP	183 – 202	Antisense	5'-**J**-CAAGCTTCCCGTTCTCAGCC-**T**-3'

[a]Numbers indicate nucleotide position of the ORF26 and GAPDH sequence.
[b]**F**, **FAM** reporter dye; **T**, **TAMRA** quencher dye; **J**, **Joe** reporter dye.

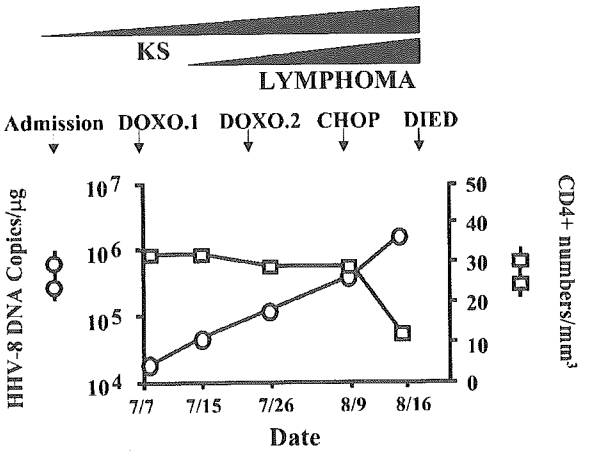

FIGURE 1 The relationship between HHV-8 viral load in whole blood cells and CD4 + cell counts on the one hand, and clinical course on the other in an HHV-8-associated solid lymphoma patient with AIDS-KS. DOXO.1: first administration of Liposomal Doxorubicin. DOXO.2: second administration of Liposomal Doxorubicin.

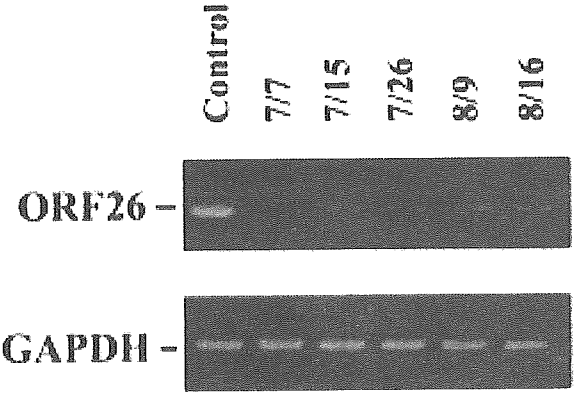

FIGURE 2 Specific amplification of real-time PCR products corresponding to HHV-8-encoded ORF26 gene and GAPDH internal control was confirmed by gel electrophoresis. The control was BCBL-1 (a B cell line derived from body-cavity-based lymphoma, which is latently infected with HHV-8) derived DNA. 7/7, 7/15, 7/26, 8/9 and 8/16 represent dates when whole blood cells were obtained from the patient.

with a 12-day interval. During treatment, right axillary and left cervical lymph nodes grew to 2 and 3–5 cm in diameter, respectively. The HHV-8 viral load was increased to 4.7×10^4 copies/μg shortly after the first course of treatment. Examination of biopsy material from these lymph nodes showed large cell lymphoma morphology, and the lymphoma spread rapidly to the eyelids, neck and arms, which appeared as growing lymphadenopathy. The HHV-8 viral load increased to 1.3×10^5 copies/μg during the first week after the second treatment course. Since the rapidly progressive lymphoma did not respond to liposomal doxorubicin, a CHOP regimen consisting of prednisolone (120 mg), doxorubicin (30 mg; reduced by 30% due to the co-existing thrombocytopenia), vincristine (2 mg, reduced by 7.4%) and cyclophosphamide (750 mg, reduced by 50%) was administered. However, the level of HHV-8 continued to increase to 3.9×10^5 copies/μg in a blood sample obtained a few days after CHOP administration, while the CD4 + cell counts remained low (29/μl). The patient died 6 days after the induction of the CHOP regimen. In the final sample obtained 2 days before the patient died, the HHV-8 viral load was 1.6×10^6 copies/μg, and the CD4 + cell counts were reduced to 12/μl. In addition, neither effusion lymphoma nor lymphocytic leukemia was detected in this patient during the whole clinical course. Overall, the HHV-8 DNA load in the whole blood cells increased by a factor of about 100 despite the therapy for KS, while the CD4 + cell counts stayed low during the progression of the lymphoma (Fig. 1). All of the real-time PCR products were confirmed as specific and the amplified product was verified as correct by acrylamide gel electrophoresis (Fig. 2).

Immunohistochemical Studies

Immunohistochemistry was performed as described previously [14]. After endogenous peroxidase was blocked with methanol-0.6% H_2O_2 for 30 min at room temperature, the anti-ORF50 or anti-ORF59 polyclonal antibodies were allowed to react at 4°C. Immunohistochemical staining showed that lymphoma cells expressing HHV-8 encoded ORF50 and ORF59 (Fig. 3a,b) antigens in the cells' nuclei. This finding suggests that HHV-8 replication did occur in the tumor mass of this patient.

DISCUSSION

Our observation of a nearly 100-fold increase of the HHV-8 DNA load in whole blood cells within 40 days and the detection of HHV-8 lytic protein in the lymphoma cells indicate that HHV-8 replicates in HHV-8-associated solid lymphoma with AIDS-associated KS. HHV-8 is etiologically associated with KS, primary effusion lymphoma (PEL) and multicentric Castleman's disease (MCD). The HHV-8-associated solid lymphoma has recently been proposed as a new type of lymphoma. It is a solid lymphoma and is often complicated with other HHV-8-associated diseases such as KS [8]. HHV-8 usually establishes latent infection in the natural host cells. Activation of HHV-8 replication in the latently infected cells, reflecting an increase in HHV-8 DNA load, is responsible for viral spread and presumed to contribute to the development of HHV-8-associated diseases [15]. It has been reported that detection of HHV-8 DNA in PBMC from HIV type 1-infected persons is associated with an increased risk of subsequent development of KS [4,5] and with KS disease progression [5,6]. Some studies have suggested quantification of the HHV-8 viral load might be useful for monitoring the therapeutic response of patients with HHV-8-associated diseases [16]. Poor prognosis is common among cases of HHV-8-associated lymphoma. Liposomal doxorubicin and the CHOP regimen are first-line agents for the treatment of KS

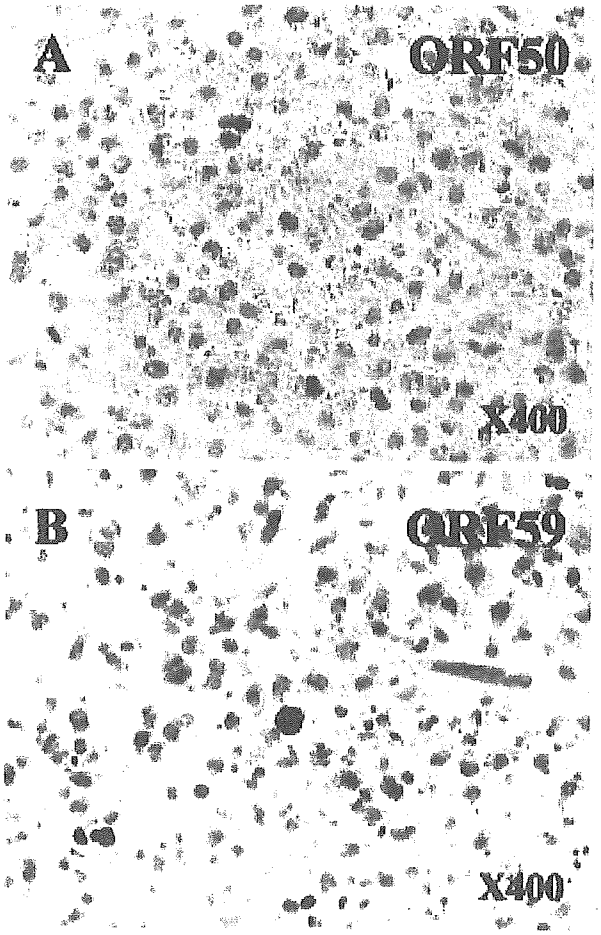

FIGURE 3 Immunohistochemical staining showed that the lymphoma cells of this patient expressed HHV-8 encoded ORF50 (A) and ORF59 (B) antigens in the cells' nuclei. Specimens were obtained at autopsy.

and lymphoma, but were not able to suppress the progression of the disease in our patient, as evidenced by the nearly 100-fold increase in the HHV-8 viral load during the 40 days of chemotherapy, and by the rapid lymphoma progression. The clinical deterioration seen in our patient accompanied by the increase in the HHV-8 viral load suggests that HHV-8 replication had occurred in this patient, and that HHV-8 had been involved in lymphoma progression. Our finding that detection of high load HHV-8 DNA is associated with lower CD4 + cell counts is consistent with data reported by others [4], providing further evidence that advanced immunosuppression is responsible for HHV-8 replication and development of lymphoma as well as KS. Co-infection with HIV may also affect HHV-8 replication and HHV-8-associated disorders through cytokine production and HIV-1 Tat protein secretion from HIV-infected cells [17–19]. Interferon γ (IFNγ) and oncostatin M (OSM) reportedly induce HHV-8 replication [20–21]. We have found that IL-6 activates HHV-8 replication in PEL-derived BCBL-1 cells [15]. In addition, EBV coinfection reported in most cases of HHV-8-associated solid lymphoma suggests HHV-8 may act in conjunction with EBV in the progression of lymphoma. However, our previous publication of this case suggested that HHV-8, rather than EBV, is the main viral agent associated with the pathogenesis of lymphoma in the patient [12]. EBV co-infection found in our patient probably contributed to the progression of HIV infection and the loss of functional immune responses.

In summary, our results suggest that the HHV-8 viral load in whole blood cells measured by real-time quantitative PCR may be useful for monitoring the response to therapies used to treat HHV-8-associated diseases. Further investigation is needed to identify the precise role of HHV-8 as well as inflammatory cytokines in HHV-8-associated solid lymphoma.

Acknowledgements

This work was supported by Grant H-12-AIDS-004 from the Ministry of Health, Labour and Welfare of Japan. We wish to thank Drs N. Nishimoto, M. Sugimoto, K. T. Nishikawa and T. Isobe for their thoughtful advice, Ms. K. Umetani for her technical assistance, and Ms. A. Okajima for secretarial assistance.

References

[1] Chang, Y., Cesarman, E., Pessin, M.S., Lee, F., Culpepper, J., Knowles, D.M., *et al.* (1994) "Identification of herpesvirus-like DNA sequences in AIDS-associated Kaposi's sarcoma", *Science*, **266**, 1865–1869.

[2] Said, J.W., Tasaka, T., Takeuchi, S., Asou, H., de Vos, S., Cesarman, E., *et al.* (1996) "Primary effusion lymphoma in woman: report of two cases of Kaposi's sarcoma herpesvirus-associated effusion-based lymphoma in human immunodeficiency virus-negative woman", *Blood*, **88**, 3124–3128.

[3] Kikuta, H., Itakura, O., Ariga, T. and Kobayashi, K. (1997) "Detection of human herpesvirus 8 DNA sequences in peripheral blood mononuclear cells of children", *Journal of Medical Virology*, **53**, 81–84.

[4] Whitby, D., Howard, M.R., Tenant-Flowers, M., Brink, N.S., Copas, A., Boshoff, C., *et al.* (1995) "Detection of Kaposi's sarcoma associated herpes virus in peripheral blood of HIV-infected individuals and progression to Kaposi's sarcoma", *Lancet*, **346**, 799–802.

[5] Campbell, T.B., Borok, M., Gwanzura, L., MaWhinney, S., White, I.E., Ndemera, B., *et al.* (2000) "Relationship of human herpesvirus 8 peripheral blood virus load and kaposi's sarcoma clinical stage", *AIDS*, **14**, 2109–2116.

[6] Cattani, P., Capuano, M., Lesnoni La Parola, I., Guido, R., Santangelo, R., *et al.* (1998) "Human herpesvirus 8 in Italian HIV-seronegative patients with Kaposi sarcoma", *Archives of Dermatology*, **134**, 695–699.

[7] Cesarman, E., Chang, Y., Moore, P.S., Said, J.W. and Knowles, D.M. (1995) "Kaposi's sarcoma-associated herpesvirus-like DNA sequences in AIDS-related body-cavity-based lymphomas", *New England Journal of Medicine*, **332**, 1186–1191.

[8] Katano, H., Suda, T., Morishita, Y., Yamamoto, K., Hoshino, Y., Nakamura, K., *et al.* (2000) "Human herpesvirus8-associated solid lymphoma occurring in AIDS patients take anaplastic large cell morphology", *Modern Pathology*, **13**, 77–85.

[9] Oksenhendler, E., Boulanger, E., Galicier, L., Du, M.Q., Dupin, N., Diss, T.C., *et al.* (2002) "High incidence of Kaposi sarcoma-associated herpesvirus-related non-Hodgkin lymphoma in patients with HIV infection and multicentric Castleman disease", *Blood*, **99**, 2331–2336.

[10] DePond, W., Said, J.W., Tasaka, T., de Vos, S., Kahn, D., Cesarman, E., *et al.* (1997) "Kaposi's sarcoma-associated herpesvirus and human herpesvirus 8 (KSHV HHV8)-associated lymphoma of the bowel. Report of two cases in HIV-positive men with secondary effusion lymphomas", *American Journal of Surgical Pathology*, **21**, 719–724.

[11] Buske, C., Hannig, H., Hiddemann, W. and Bodemer, W. (1997) "Human herpesvirus-8 (HHV-8) DNA associated with anaplastic large cell lymphoma of the B-cell type in an HIV-1-positive patient", *International Journal of Cancer*, **73**, 303–304.

[12] Yamamoto, Y., Teruya, K., Katano, H., Niino, H., Yasuoka, A., Kimura, S., *et al.* (2003) "Rapidly progressive human herpesvirus 8-associated solid lymphoma in a patient with AIDS-associated Kaposi sarcoma", *Leukemia & Lymphoma*, **44**, 1631–1633.

[13] White, I.E. and Campbell, T.B. (2000) "Quantitation of cell-free and cell-associated Kaposi's sarcoma-associated herpesvirus DNA by real-time PCR", *Journal of Clinical Microbiology*, **38**, 1992–1995.

[14] Katano, H., Sato, Y., Kurata, T., Mori, S. and Sata, T. (2000) "Expression and localization of human herpesvirus 8-encoded proteins in primary effusion lymphoma, Kaposi's sarcoma, and multicentric Castleman's disease", *Virology*, **269**, 335–344.

[15] Song, J., Ohkura, T., Sugimoto, M., Mori, Y., Inagi, R., Yamanishi, K., *et al.* (2002) "Human interleukin-6 induces human herpesvirus-8 replication in a body cavity-based lymphoma cell line", *Journal of Medical Virology*, **68**, 404–411.

[16] Tedeschi, R., Enbom, M., Bidoli, E., Linde, A., De Paoli, P. and Dillner, J. (2001) "Viral load of Human herpesvirus in peripheral blood of Huam immunodeficiency virus-infected patients with Kaposi's sarcoma", *Journal of Clinical Microbiology*, **39**, 4269–4273.

[17] Ensoli, B., Barillari, G. and Gallo, R.C. (1992) "Cytokines and growth factors in the pathogenesis of AIDS-associated Kaposi's sarcoma (Review)", *Immunological Reviews*, **127**, 147–155.

[18] Harrington, W.J., Sieczkowski, L., Sosa, C., Chan-a-Sue, S., Cai, J.P., Cabral, L., *et al.* (1997) "Activation of HHV-8 by HIV-1 tat", *Lancet*, **349**, 774–775.

[19] Varthakavi, V., Browning, P.J. and Spearman, P. (1999) "Human immunodeficiency virus replication in a primary effusion lymphoma cell line stimulates lytic-phase replication of Kaposi's sarcoma-associated Herpesvirus", *Journal of Virology*, **73**, 10329–10338.

[20] Blackbourn, D.J., Fujimura, S., Kutzkey, T. and Levy, J.A. (2000) "Induction of human herpesvirus-8 gene expression by recombinant interferon gamma", *AIDS*, **14**, 98–99.

[21] Mercader, M., Taddeo, B., Panella, J.R., Chandran, B., Nickoloff, B.J. and Foreman, K.E. (2000) "Induction of HHV-8 lytic cycle replication by inflammatory cytokines produced by HIV-1-infected T cells", *American Journal of Pathology*, **156**, 1961–1971.

Simvastatin induces apoptosis of Epstein–Barr virus (EBV)-transformed lymphoblastoid cell lines and delays development of EBV lymphomas

Harutaka Katano, Lesley Pesnicak, and Jeffrey I. Cohen*

Medical Virology Section, Laboratory of Clinical Infectious Diseases, National Institute of Allergy and Infectious Diseases, National Institutes of Health, Bethesda, MD 20892

Edited by Bernard Roizman, University of Chicago, Chicago, IL, and approved February 4, 2004 (received for review August 11, 2003)

Simvastatin and pravastatin are inhibitors of 3-hydroxy-3-methylglutaryl CoA reductase, and are used as antihypercholesterolemia drugs. Simvastatin, but not pravastatin, binds to the inserted domain of leukocyte function antigen (LFA)-1 and inhibits the function of LFA-1, including adhesion and costimulation of lymphocytes. Epstein–Barr virus (EBV)-transformed lymphoblastoid cell lines (LCLs) express high levels of LFA-1 on their surface and grow in tight clumps. Here we show that simvastatin (2 μM) inhibits clump formation and induces apoptosis of EBV-transformed LCLs. The apoptosis-inducing effect of simvastatin depends on binding to the inserted domain of LFA-1. Simvastatin, but not pravastatin, dissociates EBV latent membrane protein 1 from lipid rafts of LCLs, resulting in down-regulation of nuclear factor κB activity and induction of apoptosis. Analysis of multiple EBV-positive and -negative cell lines indicated that both LFA-1 and EBV latent membrane protein 1 expression were required for simvastatin's effects. Administration of simvastatin to severe combined immunodeficiency mice followed by inoculation with LCLs resulted in delayed development of EBV lymphomas and prolonged survival of animals. To our knowledge, this is the first report in which a drug that targets LFA-1 has been used to treat B cell lymphoma. These data suggest that simvastatin may have promise for treatment or prevention of EBV-associated lymphomas that occur in immunocompromised persons.

Infection of primary B cells with Epstein–Barr virus (EBV) results in transformation with growth of the cells in tight clumps and immortalization of the cells. These immortalized B cells have an immunoblastic morphology and express each of the EBV nuclear antigens (EBNAs) and latent membrane proteins (LMPs) (1, 2). EBNA-2 is a transactivator that up-regulates expression of cellular genes and LMPs. LMP-1 is an oncoprotein that constitutively activates nuclear factor κB (NF-κB) to induce B cell proliferation (3). LMP-1 also induces expression of adhesion molecules leukocyte function antigen (LFA)-1, LFA-3, and intercellular adhesion molecule 1 (ICAM-1) on the surface of EBV-transformed B cells (4, 5). The high level expression of adhesion molecules contributes to clumping of EBV-infected B cells *in vitro* (6).

EBV-associated immunoblastic lymphomas occur in immunocompromised patients such as those with AIDS or transplant recipients (7, 8). Because these EBV-associated immunoblastic lymphomas express each of the EBNAs and LMPs (8) that induce proliferation of B cells, the virus is thought to be directly responsible for the pathogenesis of these tumors (3). LMP-1 in EBV-associated lymphoma cells binds to tumor necrosis factor receptor-associated factors, and the tumors show activation of NF-κB (9). Many immunocompromised patients with EBV-associated immunoblastic lymphoma have tumors at extranodal sites such as the brain, lung, or gastrointestinal tract. The high-level expression of LFA-1 and other cellular adhesion molecules in these tumors may contribute to their extranodal location (10). The prognosis of these lymphomas is often poor for patients with irreversible immunosuppression, and treatment options are limited.

Simvastatin is a member of the statin family of drugs that inhibit 3-hydroxy-3-methylglutaryl CoA reductase (11). Statins lower plasma cholesterol levels, resulting in reduction of the risk of cardiovascular disease (12). Weitz-Schmidt *et al.* (13) demonstrated that certain statins, including simvastatin and lovastatin, bind to the I (inserted) domain of LFA-1 and inhibit its function (13). In contrast, other statins such as pravastatin do not bind to LFA-1. LFA-1 is expressed on the surface of various leukocytes and plays an important role in cell adhesion and costimulation of T cells. The I domain of LFA-1 is the binding site for ICAM-1, a ligand of LFA-1 (14, 15). The binding of simvastatin or lovastatin to the LFA-1 I domain induces a conformational change in LFA-1, resulting in inhibition of the interaction of LFA-1 with ICAM-1 (13). As a result of their binding to LFA-1, these statins inhibit the costimulatory activity of LFA-1 and suppress the inflammatory response in a murine model of peritonitis (13).

Here, we investigate the ability of simvastatin to inhibit EBV-positive B cell proliferation. Because simvastatin binds to and inhibits the function of LFA-1, we postulated that the drug would inhibit the growth of these cells both *in vitro* and *in vivo*. Inoculation of EBV-transformed lymphoblastoid cell lines (LCLs) into severe combined immunodeficiency (SCID) mice results in the formation of EBV-associated immunoblastic lymphomas that contain EBV genomes and express EBNAs, LMPs, and adhesion molecules including LFA-1 (16, 17). In the present study, we treated EBV-transformed LCLs *in vitro* with simvastatin, and administered the drug and inoculated SCID mice with LCLs to assess development of B cell lymphomas.

Materials and Methods

Cell Culture and Viability Assay. Three EBV-transformed LCLs, 12A1, 6B10, and 295H, EBV-positive Burkitt lymphoma cell lines [P3HR-1 (18), Akata (19), Mutu-1 (20), and Mutu-3 (20)], a human herpesvirus-8-positive EBV-negative primary effusion lymphoma cell line (BCBL-1) (21), an EBV-negative Burkitt lymphoma cell line (BJAB) (22), and EBV-negative T cell lines [Jurkat (23) and II-23 (24) cells; obtained from Carl Ware, La Jolla Institute for Allergy and Immunology, San Diego] were tested. For cell proliferation and viability assays, 2×10^4 cells per ml were cultured in 12- or 24-well plates for 5–7 days. Cell viability was assessed with XTT (Cell Proliferation Kit II, Roche Molecular Biochemicals), trypan blue, or propidium iodide (PI) staining. For PI staining, cells were washed with PBS, PI (5 μg/ml) was added, cells were washed, and fluorescent intensity was assessed with flow cytometry. Percent cell death was determined by the ratio of PI-positive cells to all gated cells.

This paper was submitted directly (Track II) to the PNAS office.

Abbreviations: EBV, Epstein–Barr virus; ICAM-1, intercellular adhesion molecule 1; I domain, inserted domain; LCL, lymphoblastoid cell line; LFA, leukocyte function antigen; LMP, latent membrane protein; PI, propidium iodide; SCID, severe combined immunodeficiency.

*To whom correspondence should be addressed at: Laboratory of Clinical Infectious Diseases, National Institutes of Health, 10 Center Drive, Building 10, Room 11N228, Bethesda, MD 20892. E-mail: jcohen@niaid.nih.gov.

www.pnas.org/cgi/doi/10.1073/pnas.0305149101

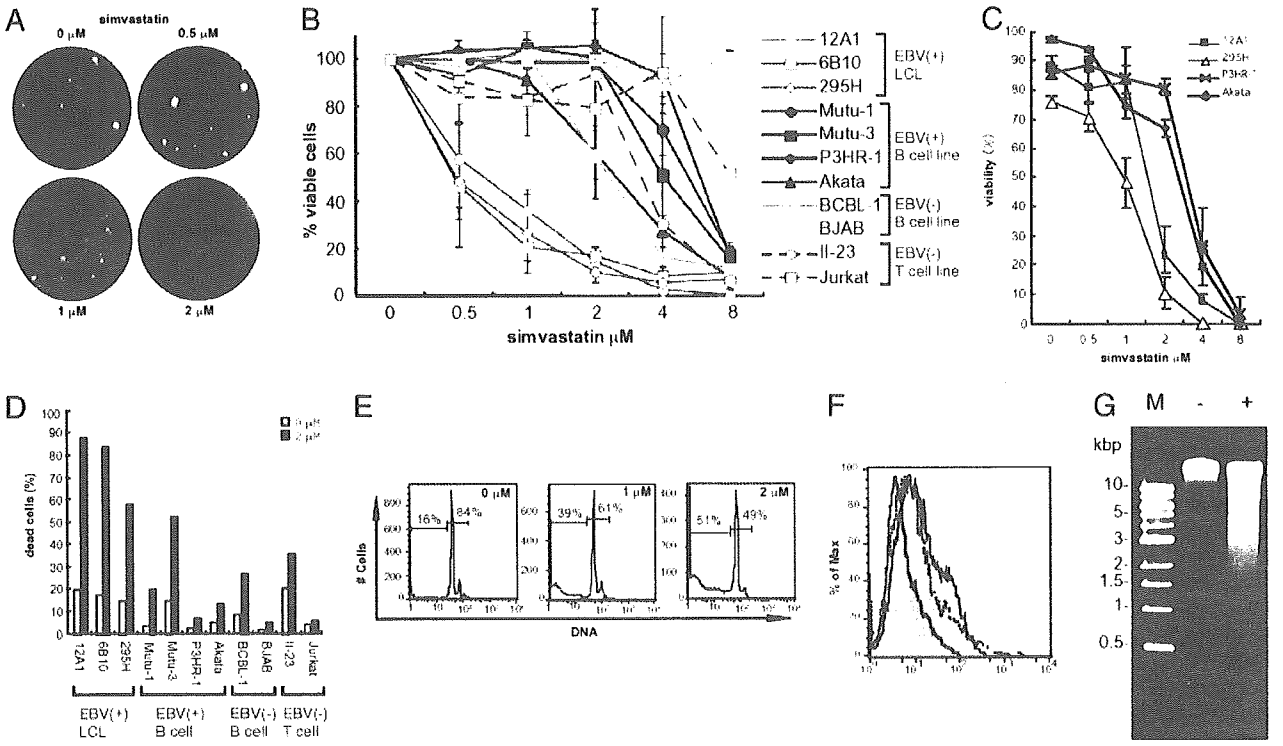

Fig. 1. Simvastatin inhibits clump formation and induces apoptosis in LCLs. (*A*) Cell clumping of LCLs was observed after simvastatin was added at 0–2 μM for 5 days. (*B*) XTT cell proliferation assay was performed after addition of simvastatin (0–8 μM) to various cells lines for 7 days. Error bars indicate standard deviations for four independent experiments. (*C*) Cell viability was assayed by trypan blue staining after cell lines were cultured with 0–8 μM simvastatin for 7 days. Error bars indicate standard deviations for three separate experiments. (*D*) Percentage of dead cells in the absence (open bars) or presence (filled bars) of 2 μM simvastatin for 7 days as determined by PI staining and flow cytometry. PI-positive cells were counted as dead cells. (*E*) PI staining. Cells were treated with or without simvastatin for 5 days. Cell populations in sub-G_0–G_1 and G_0–G_1–S–M phase are indicated. (*F*) TUNEL assays were performed for cells treated with 2 μM simvastatin for 5 days (gray area with solid line), no simvastatin for 5 days (white area with solid line), or serum starvation for 72 h (white area with dotted line). (*G*) DNA ladder formation for cells cultured with (+) or without (−) 2 μM simvastatin for 5 days.

Reagents and Antibodies. Simvastatin and pravastatin (Calbiochem) were converted to their open acid forms before use *in vitro* (25). Soluble ICAM-1 was purchased from R & D Systems. LFA-1 antibodies TS1/22 (American Type Culture Collection) (26) and G25.2 (BD Pharmingen) were used as primary antibodies, and fluorescein isothiocyanate (FITC)-conjugated $F(ab')_2$ fragment of goat anti-mouse Ig (Caltag, Burlingame, CA) was used as the secondary antibody for immunofluorescence and flow cytometry. TS1/22 antibody was obtained from hybridoma cells.

Lipid Raft Studies. Detergent extraction and flotation assay for lipid rafts were performed as described (27). Immunoblotting was performed by using anti-LMP-1 monoclonal antibody (S-12, BD Pharmingen), anti-CD71 monoclonal antibody (Zymed), and anti-Lyn monoclonal antibody (Santa Cruz Biotechnology).

Table 1. Protein expression, activation of NF-κB, and cell death induced by simvastatin in cell lines

Cell line	Description	Clumping formation	LFA-1*	ICAM-1*	EBV†	LMP-1‡	NF-κB‡	Cell death by simvastatin§
12A1	LCL	++	++	++	+	+++	++	+
6B10	LCL	++	++	++	+	+++	+++	+
295H	LCL	+	+	++	+	+++	+++	+
Mutu-1	B cell line (BL)	−	−	−	+	−	−	−
Mutu-3	B cell line (BL)	+	+	++	+	+	+	+
P3HR-1	B cell line (BL)	−	++	++	+	−	+	−
Akata	B cell line (BL)	−	−	−	+	−	+	−
BCBL-1	HHV-8-positive cell	−	−	+	−	−	−	−
BJAB	B cell line (BL)	−	+	++	−	−	−	−
II-23	T cell line	−	++	+	−	−	+	−
Jurkat	T cell line	−	−	+	−	−	−	−

*Expression levels of LFA-1 and ICAM-1 were determined with flow cytometry (Fig. 5).
†EBV-positive cells lines are indicated in refs. 18–24.
‡Expression level of LMP-1 and constitutive activation of NF-κB were determined by immunoblot and gel shift assay, respectively (Fig. 5).
§Cell death induced by 2 μM simvastatin is defined as >50% cell death by PI staining (Fig. 1*D*). BL, Burkitt lymphoma; HHV-8, human herpesvirus 8.